


Relative Helix–Helix Conformations in Branched Aromatic Oligoamide Foldamers

Nicolas Delsuc,^{†,§} Stéphane Massip,[‡] Jean-Michel Léger,[‡] Brice Kauffmann,[†] and Ivan Huc^{*,†}

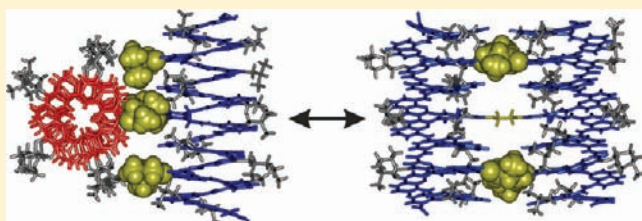
[†]Institut Européen de Chimie et Biologie, Université de Bordeaux—CNRS UMR5248 and UMS3033, 2 rue Robert Escarpit, 33607 Pessac, France

[‡]Université de Bordeaux—EA4138 Pharmacochimie, 146 rue Léo Saignat, 33076 Bordeaux, France

 Supporting Information

ABSTRACT: The de novo design and synthesis of large and well-organized, tertiary-like, α -peptidic folded architectures is difficult because it relies on multiple cooperative interactions within and between secondary folded motifs of relatively weak intrinsic stability. The very stable helical structures of oligoamides of 8-amino-2-quinoline carboxylic acid offer a way to circumvent this difficulty thanks to their ability to fold into predictable and stable secondary motifs. Branched architectures comprised of

two pairs of tetrameric (1), pentameric (2), or octameric (3) oligomers connected *via* an ethylene glycol spacer were designed and synthesized. The short spacer holds two helices in close proximity, thus enabling interactions between them. Degrees of freedom allowed in the system are well-defined: the relative *P* or *M* handedness of the two helices; the relative orientation of the helix axes; and the *gauche* or *anti* conformation of the ethylene spacer. Investigating the structures of 1–3 in the solid state and in solution allowed a detailed picture to be drawn of their conformational preferences and dynamics. The high variability of the solid state structures provides many snapshots of possible solution conformations. Helix–helix handedness communication was evidenced and shown to depend both on solvent and on a defined set of side chains at the helix–helix interface. Interdigitation of the side chains was found to restrict free rotation about the ethylene spacer. One solid state structure shows a high level of symmetry and provides a firm basis to further design specific side chain/side chain directional interactions.



INTRODUCTION

More than a decade of foldamer research has uncovered a great variety of synthetic oligomers capable of adopting well-defined folded conformations resembling the secondary folded motifs of biopolymers—helices, linear strands, or turns.¹ Parameters such as backbone shape and rigidity, local conformational preferences, specific interactions between monomers remote in a sequence, and the action of external forces such as solvent-induced forces or binding to molecules or ions may be combined to elicit a propensity to fold in a molecular strand. Biopolymers, however, rely not on secondary but mostly on tertiary folded motifs to mediate their functions. In comparison, little is achieved by isolated secondary folded elements. A great challenge for foldamer research and for chemistry in general is thus to establish design principles and synthetic methods to prepare very large and complex, yet well-organized, molecular architectures comprised of several secondary folded blocks. In recent years, examples of foldamers with tertiary-like or quaternary-like structures have begun to appear and validate the viability of this approach. As expected, faster progress has been made with foldamers that closely resemble α -peptidic structures, and in particular helix bundles. Indeed, many examples exist of artificial α -helix bundles in which several α -helices are linked to a scaffold which templates the folding of the helices upon each other.^{2–4} Thus, cyclic and non-cyclic peptidic^{5–7} and non-peptidic^{8–13} scaffolds as well as metal complexes^{14–16} have been used for this purpose.

An inherent difficulty of designing artificial tertiary or quaternary structures based on α -peptides is associated with the relatively weak stability of their secondary folded motifs when isolated from a tertiary fold. For example, α -helix bundles are typically proven by a circular dichroism signal characteristic of α -helices, whereas the individual peptide sequences that make up the bundle display little or no α -helicity when isolated. The folding of a tertiary structure thus involves multiple cooperative processes, but these processes are difficult to predict and to design. Crucial steps to circumvent this difficulty have recently been made through the mimicking of α -helix bundles using sequences composed of β -amino acids, eventually leading to hybrid α/β sequences^{17,18} and to the first protein-like objects at the exclusion of any α -amino acid.^{19–25} Among other features, β -amino acids impart stability to each separate secondary folded motif and make the overall assembly process more robust.

Opportunities are also offered by abiotic (i.e., non-peptidic) structures and, in particular, aromatic amide foldamers.^{26–28} Some aromatic amide foldamers adopt extremely stable helically folded conformations with energy barriers toward the unfolded state larger than $100 \text{ kJ} \cdot \text{mol}^{-1}$.²⁹ The structural integrity of these helices is very high and would not be a concern upon their assembly into a tertiary fold. They thus represent well suited tools

Received: November 28, 2010

Published: February 09, 2011

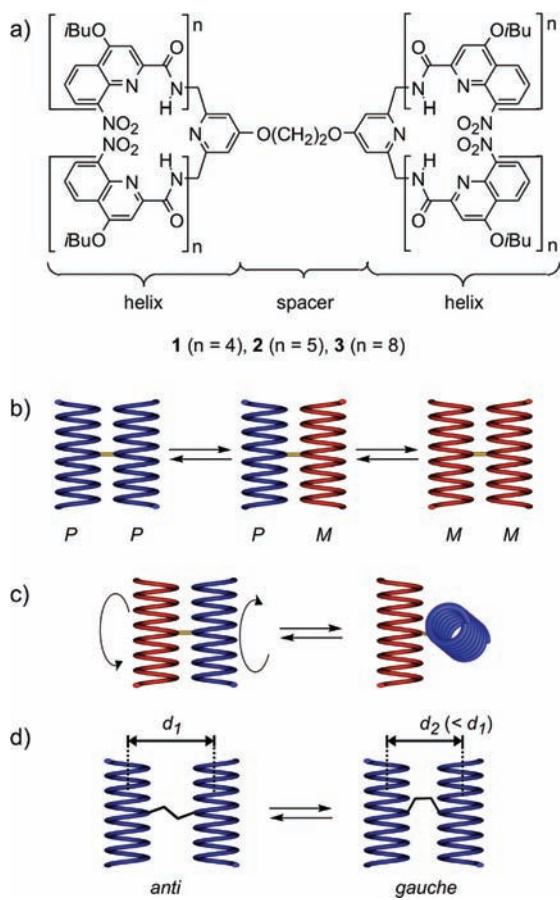


Figure 1. Formula of compounds 1–3 (a) and schematic representation of the various conformational equilibria that they may undergo: (b) Helix handedness inversion. Right-handed helices are shown in blue and left-handed helices are shown in red. (c) Rotation about the ethylene glycol spacer between helices resulting in various relative helix orientations. (d) Anti or gauche conformation of the spacer which results in different helix–helix distances.

for the modular construction of tertiary structures. For example, rigid linkers have been proposed to connect two helically folded oligomers end to end and locally predefine their relative orientation.^{30–32} Such structures, however, do not involve extensive contacts between the helices other than locally at their termini, and are thus hardly comparable to tertiary motifs. In the absence of straightforward strategies to connect two or more aromatic amide helices in a way that would force them to fold upon each other and form a defined tertiary structure, we envisaged to impose contacts between them by using a short spacer as a connection, not at their termini but in the middle of their sequences.³³ Compound 3 was designed and prepared for this purpose (Figure 1). Its branched architecture permits a convergent synthetic approach and endows it with symmetry, resulting in a relatively simple ¹H NMR spectrum and an expectedly enhanced propensity to crystallize. Although symmetry was also expected to result in NMR signal degeneracy that would hamper extensive solution studies, it was deliberately (and successfully) included in the design. The folded structure of 3 in solution was reliably predicted to consist of two multiturn helices connected at their central pyridine unit by a short ethylene glycol spacer.³³ The short spacer ensures that the two helices remain close in space but does not completely control the overall

structure, which still possesses several degrees of freedom. The first degree is related to the handedness of each helix of 3. Since 3 possesses no stereogenic center, each of its helices may have *P* or *M* helicity, and the whole molecule may exist under two distinct forms: a racemic pair *PP/MM* when the two helices have the same handedness or a *meso* species when the two helices have opposite handedness (*PM* and *MP* are degenerate). These various conformations equilibrate upon the unfolding of one helical segment and the refolding with an opposite handedness (Figure 1b). A second degree of freedom of the conformation of 3 is the relative orientation of its two helical segments, i.e., the angle between the two helix axes that may vary upon rotation at the ethylene glycol spacer (Figure 1c). A third degree of freedom is the *gauche* or *anti* conformation of the ethylene glycol spacer, which sets the interhelix distance (Figure 1d). All of these parameters may, or may not, be biased depending on the strength of the interactions between the two helical segments and their isobutoxy side chains; these were selected because they impart both a high solubility in some organic solvents and a high crystallinity.

In the following, we present a detailed investigation of the conformations of 3 and of its shorter analogues 1 and 2. Several crystal structures of these compounds have been obtained at high resolution, which allowed us to establish that the steric clash between a particular set of side chains results in an interdependence of the structural parameters mentioned above, i.e., interhelix distance, relative helix handedness, and relative helix orientation. The use of a short and rigid spacer to connect two helical secondary folded motifs thus emerges as a useful method to explore interactions between helices when no prior knowledge exists to predict specific attractions and repulsions. From this detailed conformational analysis, design elements may be assumed in order to further elaborate these synthetic objects. For example, side chain positions can be accurately organized to allow them to become close in space in a tertiary-like fold, even though they belong to distinct secondary elements.

RESULTS AND DISCUSSION

The branched architecture of 1–3 was expected to result in symmetry and thus in relatively simple ¹H NMR spectra. However, in quinoline-derived aromatic oligoamide foldamers, helix stability is such that handedness inversion is slow on the NMR time scale for any sequence longer than a tetramer.^{29,34,35} As a result, two different sets of NMR signals were expected for the *PP/MM* and *PM* diastereomeric species shown in Figure 1b. On the other hand, the equilibria shown in Figure 1c and d were expected to result in average signals (see below). Indeed, NMR spectra of 3 show two sets of signals that could be unambiguously assigned to the *PP/MM* and *PM* conformers after crystallographic analysis (see below).³³ Except in DMSO-*d*₆ in which *PM* and *PP/MM* isomers were found in equal amounts, their proportions substantially deviate from a 1:1 statistical mixture in a solvent dependent manner. The *PM* isomer largely dominates in CDCl₃ (93%, Figure 2c) and in CDCl₃/CD₃OD 2:3 vol/vol (80%), but proportions are inverted in toluene-*d*₈ in which the *PM* isomer amounts to only 30% of the total population (Table 1). The deviations from a statistical distribution indicate that the two helical segments interact with one another, either directly or via solvent molecules.

The first crystal structure of 3 was obtained (Figure 3a–c),³³ showing the conformation of the *PM* isomer. Upon dissolving these crystals, NMR spectra initially showed only one set of

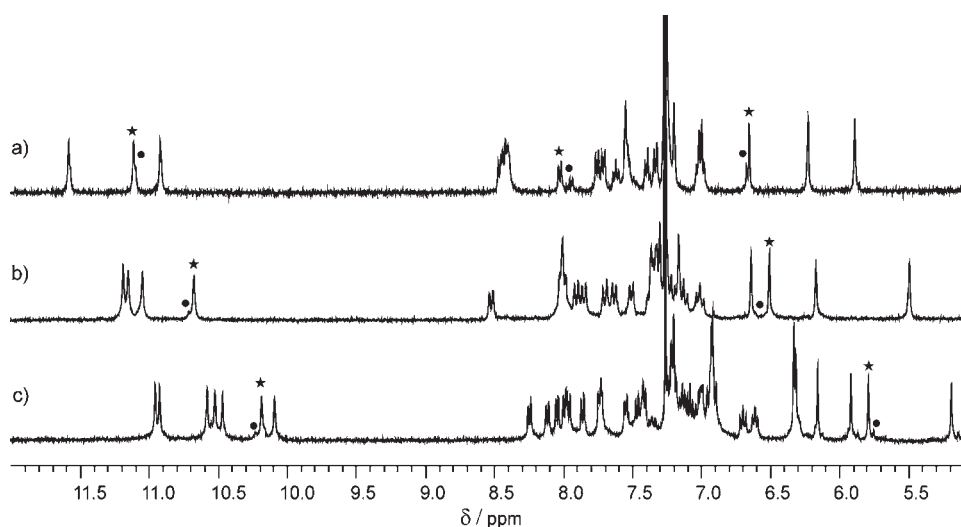


Figure 2. Part of the ^1H NMR spectra of (a) **1**, (b) **2**, and (c) **3** in CDCl_3 at 25°C showing amide (10–12 ppm) and aromatic (5–9 ppm) resonances. Most of the signals of the *PP/MM* and *PM* isomer overlap, but some can be distinguished and have been marked with a star (*PM*) or with a circle (*PP/MM*). The assignment is unambiguous in the case of **2** and **3** and tentative in the case of **1** (see text). The attribution of the signals to the two isomers and not to impurities, even when one species is a very minor component, is fully supported by the variations of proportions observed upon changing the solvent (see the Supporting Information).

Table 1. Molar Ratios of the *PP/MM* vs *PM* Isomers of **1–3 Determined by ^1H -NMR at Equilibrium**

	CDCl_3	toluene- d_8	$\text{CDCl}_3/\text{CD}_3\text{OD}$ (2:3 vol:vol)	$\text{DMSO-}d_6$
1	74/26 ^a	58/42 ^a	77/23 ^a	50/50
2	7/93	insoluble	16/84	50/50
3	7/93	70/30	20/80	50/50

^a Assignment of the two sets of NMR signals to *PM* or *PP/MM* was not possible, but it could be determined that the same species dominates in all solvents.

signals, which could be unambiguously attributed to the species observed in the solid state. The second set of signals corresponding to the *PP/MM* isomer grew over several hours as equilibrium was reached via a slow inversion of helix handedness (characteristic times: 3.5 h in toluene and 10 h in chloroform at 25°C). In the structure of the *PM* isomer of **3**, the two helical segments lie almost perpendicular (Figure 4a). The ethylene spacer adopts a *gauche* conformation, somewhat incongruous for an ethyl group having such bulky substituents, which perhaps indicates a “collapse” of the helices upon each other in the solid state. Two pairs of isobutoxy side chains lie at the helix–helix interface. They belong to the fifth quinoline rings (Q5) when counting from the C terminus of each of the four quinolinecarboxamide octamers of **3** (i.e., each Q1 unit is directly connected to a central pyridine unit). Indeed, quinolinecarboxamide has been shown to be comprised of five units per two turns.^{34,36} The isobutoxy chains of Q5 thus protrude from the helix almost exactly two turns (7 Å) above and below the ethylene glycol spacer of the central pyridine ring. The short length of the ethylene glycol spacer results in an interdigitation of the two pairs of isobutoxy chains at Q5, which appear not to easily pass each other upon rotation about the ethylene spacer (equilibrium in Figure 1c), even if the latter were in an extended (*anti*) conformation. These unavoidable direct contacts between the helices might be responsible for at least part of the interdependent helix handedness of the two helical segments. A possible mechanism for rotation

to take place about the ethylene spacer would be a local spring-like extension of two of the four quinolinecarboxamide oligomers, a phenomenon that has previously been demonstrated in other helical aromatic oligoamides in which it results in the formation of double helical dimers.³⁷ NMR did not allow us to assess this rotation in detail, since we could not determine whether the equilibrium was fast or slow on the NMR time scale, as the species before and after a 90° rotation are degenerate. On the other hand, the *gauche* to *anti* equilibrium of the ethylene spacer (Figure 1d) should result in inequivalent species but is expected to be rapid on the NMR time scale.

Another feature of the crystal structure of the *PM* isomer of **3** is that it does not possess any crystallographic or non-crystallographic symmetry element. The *gauche* conformation of the ethylene spacer results in a relative offset of the two helices along the plane of their interface, as is clearly visible in Figure 3c. This contrasts with the average symmetrical structure observed in the NMR spectra: only eight amide resonances are seen for the *PM* conformer and eight for the *PP/MM* conformer. The offset of the helices and the *gauche* conformation itself thus appear to be a snapshot among other possible conformers which equilibrate in solution. To clarify this point and also to clarify the role of the isobutoxy side chains in the Q5 rings, we extended our investigation to the shorter analogues **1** and **2**.

Compound **1** possesses four tetrameric quinolinecarboxamide oligomers. In other words, it does not have any Q5 ring and thus no side chain in the helix–helix interface. In a similar manner to **3**, the NMR spectrum of **1** in CDCl_3 shows two sets of signals (Figure 2a). Their relative proportions (74/26) indicate that one species is slightly favored but not to the same extent as for **3** in the same solvent (93:7). This ratio remains essentially unchanged in favor of the same species upon adding CD_3OD (see the Supporting Information). In toluene, a 58:42 mixture is observed, but unlike **3**, there is no inversion of proportions: the same species dominates in chlorinated and aromatic solvents. Proportions are also 50:50 in $\text{DMSO-}d_6$. Thus, it appears that helix–helix handedness communication between the two segments

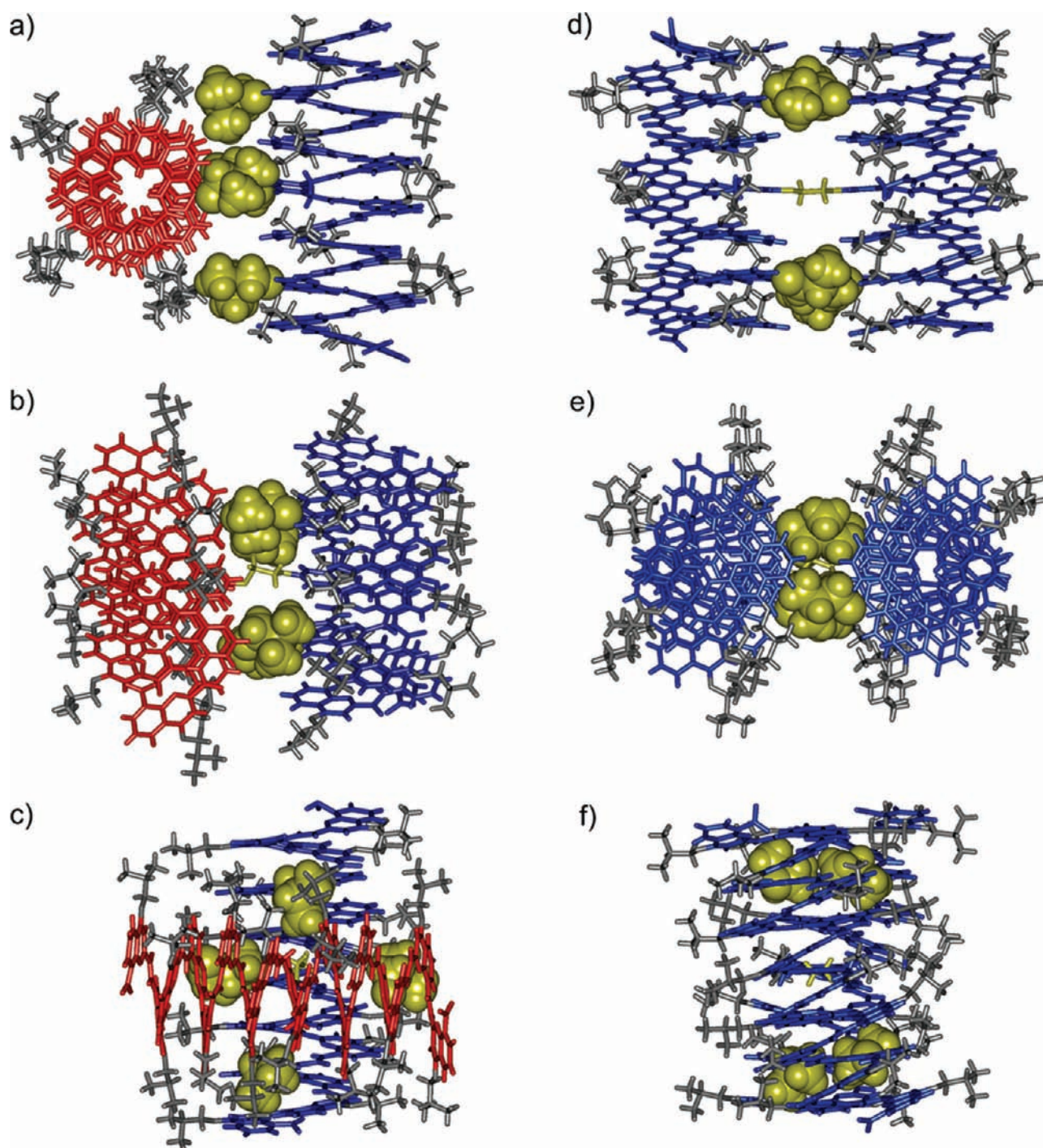


Figure 3. Structures of the *PM* isomer of **3** (a–c) and of the *PP* isomer of **3** (d–f) in the solid state shown as front views (a and d), top views (b and e), and side views (c and f). Right-handed helices are shown in blue, and left-handed helices are shown in red. Most isobutoxy side chains are shown in gray. The ethylene spacer and the four isobutoxy chains (in CPK) which lie at the interface between the helical segments are shown in yellow. Included solvent molecules are omitted for clarity.

of **1** is weaker than in **3** and that it does not depend on solvent in the same manner. A crystal structure of the *PP/MM* conformer of **1** (Figure 5b) was obtained. Unfortunately, upon redissolving these crystals, equilibrium was reached before an NMR spectrum could be measured because of the shorter helix length. We were therefore unable to assign whether the *PP/MM* conformer is the prevalent species in CDCl_3 or whether it is the minor component. This crystal structure reveals a parallel orientation of the

two helices.³⁸ This is apparently allowed by the absence of the Q5 rings which would have resulted in steric hindrance at the helix–helix interface. In a similar manner to the *PM* conformation of **3**, the ethylene spacer of **1** is in a *gauche* conformation (Figure 4d). This again results in an offset of the two helices in the plane of their interface and in the absence of symmetry of the overall structure of **1**. The recurrence of the *gauche* conformation in the solid state may be explained by the fact that it is slightly more

compact than the *anti* conformation. Because of the large volume of the helices and the apparent absence of attractive interactions between them, the *anti* conformation would be expected to dominate in solution.

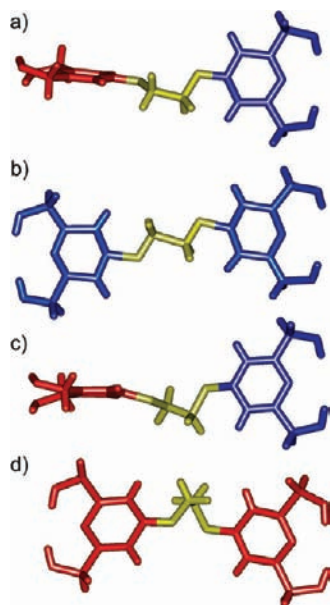


Figure 4. Part of the crystal structures of 1–3 showing the two 2,6-bis-(aminomethyl)-pyridine units linked by the ethylene glycol spacer in position 4 (in yellow). The pyridine rings are color coded according to the right (blue) or left (red) handedness of the helix to which they belong. (a) *PM* isomer of 3 possessing a torsion angle of 71.4° for the spacer and a relative angle of pyridine planes of 89.5° ; (b) *PP* isomer of 3 possessing a torsion angle of 174.1° for the spacer and a relative angle of pyridine planes of 6.9° ; (c) *PM* isomer of 2 possessing a torsion angle of 96.9° for the spacer and a relative angle of pyridine planes of 89.2° ; (d) *MM* isomer of 1 possessing a torsion angle of -58.8° for the spacer and a relative angle of pyridine planes of 38.8° .

Compound 2 differs from 1 by only one additional quinoline residue at each quinolinecarboxamide oligomer. However, it is important to note that this residue is the *QS* residue possessing the side chain which protrudes into the helix–helix interface. It is therefore logical that the solution behavior and the solid state conformation of 2 resemble more closely those of 3 than those of 1. In CDCl_3 , one isomer of 2 dominates (Figure 2b) in the same proportions as observed with 3 (93:7). As for 3, unambiguous NMR assignment of the dominant isomer of 2 to the *PM* conformer could be made by dissolving crystals (see below) and rapidly measuring a ^1H NMR spectrum. Thus, the exact match between the observed proportions of isomers in 2 and 3 is not a coincidence: it reflects the prevalence of the same species probably for the same reason. Unexpectedly, unlike 1 and 3, 2 proved to be insoluble in toluene- d_8 and in C_6D_6 , which prevented measurements in these solvents. In $\text{DMSO}-d_6$, the *PM* and *PP/MM* isomers of 2 are found in equal amounts, as for 1 and 3. The crystal structure of the *PM* isomer 2 is shown in Figure 5a. It is very similar to that of 3, with the two helices in a perpendicular orientation and the ethylene glycol spacer in a *gauche* conformation (Figure 4c). However, a slight difference which makes the two structures non-superimposable is the sign of the ethylene glycol dihedral angle, which is positive ($+71.4^\circ$) in one case and negative (-96.9°) in the other. This difference implies conformation dynamics at the ethylene glycol spacer in solution, and the absence of a strictly defined conformation imposed by the interdigitation of isobutoxy residues at *QS* (as found in peptide helix zippers and bundles).

Finally, our investigation could be completed by taking advantage of the high crystallinity of these large objects and of their dynamic behavior in solution, leading to the successful crystallization of the *PP/MM* isomer of 3 (Figure 3d–f). Crystals were grown from the same solvent system that led to the crystallization of the *PM* isomer of 3 (Figure 3a–c): liquid–liquid diffusion of methanol into a 1,2-dichloroethane solution. The *PM* isomer is the dominant species at equilibrium in this solvent. To favor the

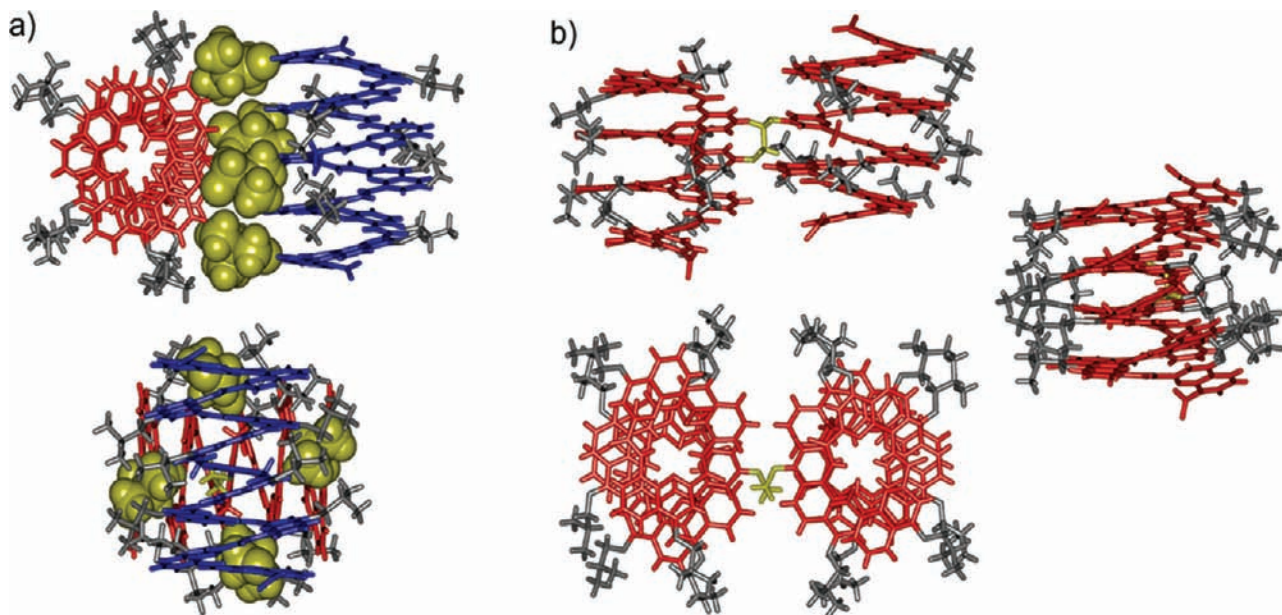


Figure 5. Structures of the *PM* isomer of 2 (a) and of the *MM* isomer of 1 (b) in the solid state. Right-handed helices are shown in blue, and left-handed helices are shown in red. Most side isobutoxy side chains are shown in gray. The ethylene spacer and the four isobutoxy chains (in CPK) which lie at the interface between the helical segments (only in part a) are shown in yellow. Included solvent molecules are omitted for clarity.

presence of a substantial amount of the *PP/MM* isomer, the sample was first brought to equilibrium in toluene, evaporated, dissolved in 1,2-dichloroethane, and immediately set to crystallize. Unlike in all other structures, the *PP/MM* isomer of **3** features an *anti* conformation of the ethylene glycol spacer (Figure 4b). This results in a slightly larger helix–helix distance, which allows an almost parallel orientation of the helices (Figure 3f). Despite this, it is evident that the isobutoxy chains cannot pass each other upon rotation about the ethylene spacer without a partial unfolding of the helices. The two

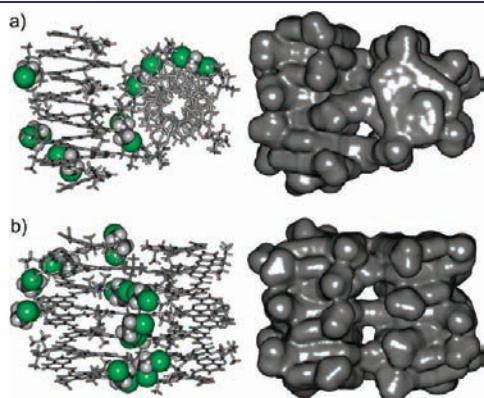


Figure 6. Solvent accessible surfaces (right) and CPK views of some of the included 1,2-dichloroethane molecules at the surface (left) of the *PM* (a) and of the *PP* (b) isomers of **3**. Chlorine atoms are shown in green. Solvent molecules more remote from the bundle surfaces have been omitted for clarity.

almost parallel helices bring their isobutoxy chains at the *QS* residues into pairwise contacts. However, it is precisely these contacts which prevent a fully parallel orientation, as seen in the structure of **1**.

Interestingly, of all the X-ray structures measured, the conformation of the *PP* isomer of **3** is the only one which adopts (non-crystallographic) symmetry elements, i.e., two perpendicular C_2 axes that cross the ethylene spacer in its middle. The high symmetry of this structure matches with that observed on average in solution. It provides a firm basis on which to design intramolecular interactions between the two helical segments, allowing enhanced helix–helix handedness communication, for example, by replacing the isobutoxy side chains at *QS* with hydrogen bonding residues.

One might have hoped that the availability of the crystal structures of both the *PM* and the *PP/MM* isomers of **3** would shed some light on the prevalence of one or the other isomer in solution. However, we could not find any obvious pattern in these structures from which to derive a rationale of the observed solution behavior. Deviations from a 50:50 mixture in solution are relatively modest (93:7 at most), and it is difficult to assign the corresponding small energy difference to structural features in such large objects. Nevertheless, the two conformations of **3** provide a qualitative illustration of the importance of the solvent in determining relative helix–helix conformation. As shown in Figure 6, the solvent accessible surfaces of both conformers are quite rough, with multiple grooves and cavities all the way throughout the structure of these objects. In the solid state, these spaces are filled with numerous 1,2-dichloroethane molecules (with very few methanol molecules in comparison), including at

Table 2. Crystallographic Data for **1–3**

	1	2	3 (PM)³³	3 (PP/MM)
solvent/precipitant	1,2 dichloroethane/ methanol	dichloromethane–toluene/ methanol	1,2 dichloroethane/ methanol	1,2 dichloroethane/ methanol
formula	C ₂₅₂ H ₃₁₆ N ₃₈ O ₆₆ Cl ₂	C ₃₁₀ H ₃₂₂ N ₄₆ O ₅₆	C ₄₈₉ H ₆₀₂ Cl ₁₂ N ₇₀ O ₁₁₈	C ₃₀₀ H ₄ Cl ₁₅ N ₁₀₀ O ₅₀
size (mm)	0.15 × 0.10 × 0.10	0.15 × 0.10 × 0.10	0.2 × 0.15 × 0.1	0.15 × 0.08 × 0.03
aspect	yellow prism	yellow prism	yellow prism	yellow plate
unit cell	triclinic	monoclinic	triclinic	triclinic
space group	<i>P</i> -1	<i>C</i> <i>c</i>	<i>P</i> -1	<i>P</i> -1
<i>Z</i>	2	4	2	2
<i>a</i> (Å)	21.925 (4)	47.509 (10)	28.1917 (13)	29.831 (3)
<i>b</i> (Å)	27.301 (5)	29.741 (6)	29.8945 (13)	33.225 (4)
<i>c</i> (Å)	28.332 (6)	33.604 (7)	36.8224 (17)	34.490 (4)
α (deg)	91.736 (6)	90.00	78.369 (3)	70.125 (10)
β (deg)	106.690 (5)	134.96 (3)	80.612 (3)	80.486 (9)
γ (deg)	97.015 (5)	90.00	71.172 (3)	63.721 (10)
temperature (K)	100 (2)	100 (2)	100 (2)	100 (2)
volume (Å ³)	16085 (5)	33599 (12)	28608 (2)	28822 (5)
FW (g·mol ⁻¹)	5004.33	5572.14	9773.80	6335.75
ρ (g·cm ⁻³)	1.023	1.067	1.135	1.163
radiation type	Synchrotron (EMBL X11)	Synchrotron (ESRF ID29)	Cu K α	Cu K α
λ (Å)	0.84900	0.85000	1.54178	1.54178
θ measured (deg)	3.48 ≤ θ ≤ 22.70	1.64 ≤ θ ≤ 29.88	6.51 ≤ θ ≤ 72.35	1.56 ≤ θ ≤ 42.35
collected reflections	182422	43588	171148	107002
used reflections (<i>I</i> > 2 Σ (<i>I</i>))	23921	21943	81044	12125
GOF	1.121	1.023	1.018	1.08
<i>R</i> ₁ (<i>I</i> > 2 Σ (<i>I</i>))	0.1861	0.1694	0.1926	0.2117
<i>wR</i> ₂ (<i>I</i> > 2 Σ (<i>I</i>))	0.4393	0.2189	0.4628	0.5216

the helix–helix interface. These probably contribute to the handedness communication between the two helical segments.

CONCLUSION

In the absence of general design principles for the folding of tertiary structures in aromatic oligoamide foldamers, we have conceived compounds **1–3** with a short connecting spacer placed in the middle of the sequences of the two helical segments. The spacer brings the helices together and limits the degrees of conformational freedom. Solution studies revealed that the conformations are on average symmetrical, in accordance with the branched architectures. In addition, it was shown that intramolecular helix handedness communication takes place via side-by-side interactions, and is probably mediated by solvent molecules. The overall rigidity of **1–3** is probably responsible for their high crystallinity, and despite their large size, several crystal structures have been obtained. Indeed, the structures of **3** belong to the largest molecules characterized by X-ray crystallography known to date that are fully synthetic, and not derived from natural products (proteins or nucleic acids). The crystal structures give an accurate sampling of the equilibria involved in the conformation of these objects. Equilibria between *PM* vs *PP/MM* conformers, parallel vs perpendicular relative orientation of the helical segments, and *gauche* vs *anti* confirmation of the ethylene glycol spacer could all be characterized in the solid state. Thus, a detailed picture of their conformation behavior in solution can be drawn from the solid state data. The value of our approach which consisted of limiting conformational freedom is that structural information about helix–helix relative conformations could be obtained even though these conformations could not be designed. In addition, the crystal structures, in particular the symmetrical structure of the *PP* conformer of **3**, provide a firm basis on which to design specific side chain/side chain interactions that may ultimately render the rigidifying element (i.e., the short ethylene glycol bridge) unnecessary for tertiary-like folding. Steps are being made in this direction and will be reported in due course.

EXPERIMENTAL SECTION

Crystal structures of compounds **1** and **2** had to be collected at synchrotron beamlines (see Table 2 for statistics). All the data collected were integrated and scaled using the XDS package.³⁹ Both structures were solved by direct methods with SHELXD.⁴⁰ Crystallographic data of compound **3** (*PP/MM*) were collected using Cu K α radiations on an Oxford Diffraction SuperNova microfocus diffractometer and processed with CrysAlisPro (Oxford diffraction). The data reported in Table 2 for compound **3** (*PM*) have been published previously.³³ The structure of compound **3** (*PP/MM*) was solved using the charge flipping algorithm implemented in Superflip.⁴¹ All structures were refined using SHELXL. The positions of the H atoms were deduced from coordinates of the non-H atoms and confirmed by Fourier synthesis. The non-H atoms were refined with anisotropic temperature parameters. H atoms were included for structure factor calculations but not refined. Since stable refinement could not be reached for compound **2** when side chain hydrogen atoms were present, we have decided to not include them in the final model.

ASSOCIATED CONTENT

S Supporting Information. Synthetic procedures, analytical and spectral characterization of **1** and **2**, and crystallographic information files (CIF). This material is available free of charge via the Internet at <http://pubs.acs.org>.

AUTHOR INFORMATION

Corresponding Author

*E-mail: i.huc@iecb.u-bordeaux.fr.

Present Addresses

^SLaboratoire des BioMolécules, UMR7203, Ecole Normale Supérieure, Département de chimie, 24 rue Lhomond, 75005 Paris, France.

ACKNOWLEDGMENT

This work was supported by an ANR grant (project no. NT05-3_44880) and by the Ministry of research (predoctoral fellowship to N.D.). We thank Dr. Yann Ferrand for his help in the preparation of Figure 1. The authors are very grateful to Dr. David Watkin from Oxford University, Dr. Manfred Weiss from EMBL Hamburg (X11), and Dr. Christoph Mueller-Dieckmann from ID29 at ESRF for beamtime and technical assistance during data collections.

REFERENCES

- (1) Hecht, S. M.; Huc, I. *Properties and Applications*; Wiley-VCH: Weinheim, Germany, 2007.
- (2) Baltzer, L.; Nilsson, H.; Nilsson, J. *Chem. Rev.* **2001**, *101*, 3153–3163.
- (3) Schneider, J. P.; Kelly, J. W. *Chem. Rev.* **1995**, *95*, 2169–2187.
- (4) Tuchscherer, G.; Grell, D.; Mathieu, M.; Mutter, M. *J. Peptide Res.* **1999**, *54*, 185–194.
- (5) Singh, Y.; Dolphin, G. T.; Razkin, J.; Dumy, P. *ChemBioChem* **2006**, *7*, 1298–1314.
- (6) Mutter, M.; Tuchscherer, G. G.; Miller, C.; Altmann, K.-H.; Carey, J. R. I.; Wyss, D. F.; Labhardt, A. M.; Rivier, J. E. *J. Am. Chem. Soc.* **1992**, *114*, 1463–1470.
- (7) Hauert, J.; Fernandez-Carneado, J.; Michielin, O.; Mathieu, S.; Grell, D.; Schapira, M.; Spertini, O.; Mutter, M.; Tuchscherer, G.; Kovacsovic, T. *ChemBioChem* **2004**, *5*, 856–864.
- (8) Akerfeldt, K. S.; Kim, R. M.; Camac, D.; Groves, J. T.; Lear, J. D.; DeGrado, W. F. *J. Am. Chem. Soc.* **1992**, *114*, 9656–9657.
- (9) Sasaki, T.; Kaiser, T. *Biopolymers* **1990**, *29*, 79–88.
- (10) Wong, A. K.; Jacobsen, M. P.; Winzor, D. J.; Fairlie, D. P. *J. Am. Chem. Soc.* **1998**, *120*, 3836–3841.
- (11) Jensen, K. J.; Brask, J. *Biopolymers* **2005**, *80*, 747–761.
- (12) Seo, E. S.; Scott, W. R. P.; Straus, S. K.; Sherman, J. C. *Chem.—Eur. J.* **2007**, *13*, 3596–3605.
- (13) Seo, E. S.; Sherman, J. C. *Biopolymers* **2007**, *88*, 774–779.
- (14) Ghadiri, M. R.; Soares, C.; Choi, C. *J. Am. Chem. Soc.* **1992**, *114*, 4000–4002.
- (15) Suzuki, K.; Hiroaki, H.; Kohda, D.; Nakamura, H.; Tanaka, T. *J. Am. Chem. Soc.* **1998**, *120*, 13008–13015.
- (16) Schnepf, R.; Haehnel, W.; Wieghardt, K.; Hildebrandt, P. *J. Am. Chem. Soc.* **2004**, *126*, 14389–14399.
- (17) Price, J. L.; Horne, W. S.; Gellman, S. H. *J. Am. Chem. Soc.* **2007**, *129*, 6376–6377.
- (18) Horne, W. S.; Johnson, L. M.; Ketas, T. J.; Klasse, P. J.; Lu, M.; Moore, J. P.; Gellman, S. H. *Proc. Natl. Acad. Sci. U.S.A.* **2009**, *106*, 14751–14756.
- (19) Cheng, R. P.; DeGrado, W. F. *J. Am. Chem. Soc.* **2002**, *124*, 11564–11565.
- (20) Sharma, G. V. M.; Subash, V.; Narsimulu, K.; Sankar, A. R.; Kunwar, A. C. *Angew. Chem., Int. Ed.* **2006**, *45*, 8207–8210.
- (21) Daniels, D. S.; Petersson, E. J.; Qiu, J. X.; Schepartz, A. *J. Am. Chem. Soc.* **2007**, *129*, 1532–1533.
- (22) Goodman, J. L.; Petersson, E. J.; Daniels, D. S.; Qiu, J. X.; Schepartz, A. *J. Am. Chem. Soc.* **2007**, *129*, 14746–14751.
- (23) Goodman, J. L.; Molski, M. A.; Qiu, J.; Schepartz, A. *ChemBioChem* **2008**, *9*, 1576–1578.

- (24) Petersson, E. J.; Schepartz, A. *J. Am. Chem. Soc.* **2008**, *130*, 821–823.
- (25) Molski, M. A.; Goodman, J. L.; Craig, C. J.; Meng, H.; Kumar, K.; Schepartz, A. *J. Am. Chem. Soc.* **2010**, *132*, 3658–3659.
- (26) Huc, I. *Eur. J. Org. Chem.* **2004**, 17–29.
- (27) Gong, B. *Acc. Chem. Res.* **2008**, *41*, 1376–1386.
- (28) Li, Z.-T.; Hou, J.-L.; Li, C. *Acc. Chem. Res.* **2008**, *41*, 1343–1353.
- (29) Delsuc, N.; Kawanami, T.; Lefeuvre, J.; Shundo, A.; Ihara, H.; Takafuji, M.; Huc, I. *ChemPhysChem* **2008**, *9*, 1882–1890.
- (30) Maurizot, V.; Dolain, C.; Leydet, Y.; Léger, J.-M.; Guionneau, P.; Huc, I. *J. Am. Chem. Soc.* **2004**, *126*, 10049–10052.
- (31) Delsuc, N.; Hutin, M.; Campbell, V. E.; Kauffmann, B.; Nitschke, J. R.; Huc, I. *Chem.—Eur. J.* **2008**, *14*, 7140–7143.
- (32) Hu, H.-Y.; Xiang, J.-F.; Yang, Y.; Chen, C.-F. *Org. Lett.* **2008**, *10*, 69–72.
- (33) Delsuc, N.; Léger, J.-M.; Massip, S.; Huc, I. *Angew. Chem., Int. Ed.* **2007**, *46*, 214–217.
- (34) Jiang, H.; Léger, J.-M.; Huc, I. *J. Am. Chem. Soc.* **2003**, *125*, 3448–3449.
- (35) Dolain, C.; Léger, J.-M.; Delsuc, N.; Gornitzka, H.; Huc, I. *Proc. Natl. Acad. Sci. U.S.A.* **2005**, *102*, 16146–16151.
- (36) Sánchez-García, D.; Kauffmann, B.; Kawanami, T.; Ihara, H.; Takafuji, M.; Delville, M.-H.; Huc, I. *J. Am. Chem. Soc.* **2009**, *131*, 8642–8648.
- (37) Berni, E.; Kauffmann, B.; Bao, C.; Lefeuvre, J.; Bassani, D. M.; Huc, I. *Chem.—Eur. J.* **2007**, *13*, 8463–8469.
- (38) This is the only structure in which the two helix axes are found in the same plane. However, they are not, strictly speaking, parallel, since they show some divergence within that plane (see Figure 4d).
- (39) Kabsch, W. *J. Appl. Crystallogr.* **1993**, *26*, 795–800.
- (40) Sheldrick, G. M. *Acta Crystallogr.* **2008**, *A64*, 112–122.
- (41) Palatinus, L.; Chapuis, G. *Appl. Crystallogr.* **2007**, *40*, 786–790.